

College of Engineering



Drexel E-Repository and Archive (iDEA)

<http://idea.library.drexel.edu/>

Drexel University Libraries

www.library.drexel.edu

The following item is made available as a courtesy to scholars by the author(s) and Drexel University Library and may contain materials and content, including computer code and tags, artwork, text, graphics, images, and illustrations (Material) which may be protected by copyright law. Unless otherwise noted, the Material is made available for non profit and educational purposes, such as research, teaching and private study. For these limited purposes, you may reproduce (print, download or make copies) the Material without prior permission. All copies must include any copyright notice originally included with the Material. **You must seek permission from the authors or copyright owners for all uses that are not allowed by fair use and other provisions of the U.S. Copyright Law.** The responsibility for making an independent legal assessment and securing any necessary permission rests with persons desiring to reproduce or use the Material.

Please direct questions to archives@drexel.edu



Ambient and 550 °C tribological behavior of select MAX phases against Ni-based superalloys

S. Gupta^a, D. Filimonov^{a,*}, V. Zaitsev^b, T. Palanisamy^c, M.W. Barsoum^a

^a Department of Materials Science and Engineering, Drexel University, Philadelphia, PA 19104, United States

^b Department of Materials Science and Engineering, State University of New York at Stony Brook, Stony Brook, NY 11794, United States

^c Honeywell International Inc., Morristown, NJ 07962, United States

Received 15 June 2006; received in revised form 6 February 2007; accepted 12 March 2007

Abstract

In this paper, we report on the tribological behavior, at 25 and 550 °C of the following layered (MAX phase) ternary carbides: Ti₂AlC, Cr₂AlC, Ta₂AlC, Ti₃SiC₂, Ti₂AlN, Ti₄AlN₃, Cr₂GeC, Cr₂GaC, Nb₂SnC and Ti₂SnC, tested against Ni-based superalloys, SA (Inconel-718 and Inconel-600). The tests were performed using a pin-on-disc method at 1 m/s and 3 N. At room temperature, the wear rates, WRs, were relatively high ($\geq 10^{-4}$ mm³/N-m) and no correlation was found between the WRs and the friction coefficients, μ . Third body abrasion is believed to be responsible for the high WRs at this temperature. At 550 °C, oxidized transfer films were identified on both contact surfaces. The tribofilms comprised mostly of Ni, Cr, Fe and O and resulted in low ($< 10^{-6}$ mm³/N-m) WRs and μ 's < 0.5 . This result implies that the tribo-oxidation products of the Ni-based SA tested herein (Inconel 718) are lubricious.

© 2007 Published by Elsevier B.V.

Keywords: MAX phases tribology; Tribofilm formation; Tribo-oxidation; Solid lubricants; Lubricious effect

1. Introduction

By now it is reasonably well established that as a class the 50+ MAX phases known to date display unusual and sometimes unique properties [1-3]. These phases are so-called because of their chemistry: M_{n+1}AX_n, where *n* is 1, 2 or 3, M is an early transition metal, A is an A-group (mostly IIIA and IVA) element, and X is either C and/or N. These compounds are layered, possess hexagonal symmetry (space group P6₃/mmc) and consist of M carbide or nitride layers interleaved with metallicity bonded A-element layers. They are highly damage tolerant, thermal shock resistant, readily machinable, and with Vickers hardness values of 2-5 GPa, are anomalously soft for transition metal carbides and nitrides. They are also excellent conductors of heat and electricity [3-6].

The MAX phases decompose incongruently in inert atmospheres into MX-based compounds and A-rich liquids. The decomposition temperatures vary from over 2000 °C to under 1000 °C [3]. In air, at elevated temperatures, however, they are

oxidized at lower temperatures [3,7,8]. Some, notably Ti₃SiC₂ and Ti₂AlC, have excellent oxidation resistances because they form protective oxide layers [3,7-9].

In the first report on the properties of Ti₃SiC₂, it was noted that the material felt lubricious [2], which led Myhra et al. to study its tribological properties using a lateral force microscope with a Si₃N₄ tip [10]. They showed that indeed the friction coefficients, μ , of the basal planes were ultra-low (2 to 5 × 10⁻³). The μ 's of non-basal planes, however, were much higher.

El-Raghy et al. [11] studied the tribology of coarse-grained, CG (≈25-50 μm) and fine-grained, FG (≈4 μm) polycrystalline Ti₃SiC₂ samples, using a pin-on-disc method and a diamond belt abrasion test. The tests were carried out using a 9.5-mm diameter 440C steel ball, a load of 5 N, with a sliding speed of 0.1 m/s. For both the microstructures, μ rose linearly from 0.15 to 0.4 and then to a steady state value of 0.8. The initial transition region was longer for the CG than the FG samples. The average sliding wear rates were high, 1.34 × 10⁻³ and 4.25 × 10⁻³ mm³/N-m for the FG and CG samples, respectively.

Sun et al. [12] studied Ti₃SiC₂ with 7 wt.% TiC against 3.5 mm steel pins, and showed that the μ 's were not very sensitive to normal load, and displayed steady state values of 0.4-0.5. The average WR was 9.9 × 10⁻⁵ mm³/N-m, and increased with

* Corresponding author. Fax: +1 2158956760.

E-mail address: filin@radio.chem.msu.ru (D. Filimonov).

load. Fine-grained, and partially compacted tribo-layers containing Fe were observed on the plane, along with ploughing of the steel pins. Zhang et al. [13] used an oscillating pin-on-disc method, with loads in the range of 1–10 N at a sliding speed of 13 mm/s, to study the tribological properties between self-mated couples of Ti_3SiC_2 and between Ti_3SiC_2 and diamond. They reported μ 's of ~ 1 to 1.5 for the former, and $\mu \sim 0.1$ for the latter. The low μ 's between Ti_3SiC_2 and diamond were attributed to the formation of a tribofilm. Zhai et al. [14] evaluated Ti_3SiC_2 against low carbon steel using a block-on-disc method at a sliding speed of 20 m/s and loads corresponding to stresses between 0.1 and 0.8 MPa. They reported that the tribofilms formed were composed of TiO_2 , SiO_2 and Fe_2O_3 .

Souchet et al. [15] also studied the tribology of FG ($\approx 4 \mu\text{m}$) and CG ($\approx 25\text{--}50 \mu\text{m}$) samples against steel and Si_3N_4 balls using a reciprocating type tribometer. Two successive wear regimes were observed for the CG and FG samples against both counterparts. During Regime I, both the WRs and μ were low. Regime I was followed by Regime II in which μ increased to 0.4–0.5 and wear became significant.

Sarkar et al. [16] studied the tribology of Ti_3SiC_2 against steel using a ball-on-disc method under fretting condition as the load was varied between 1 and 10 N. The μ 's, they obtained, varied between 0.5 and 0.55, and the WRs were between 11 and $37 \times 10^{-5} \text{mm}^3/\text{N}\cdot\text{m}$.

Hongxiang et al. [17] tested Ti_3AlC_2 using a block-on-disc method against low carbon steel. At 60 m/s rotation speed and loads corresponding to stresses of ≈ 0.8 MPa, μ was ~ 0.1 and the specific WR was $\sim 2.5 \times 10^{-6} \text{mm}^3/\text{N}\cdot\text{m}$. It was argued that self-generating tribofilms, composed of Ti, O, Al and Fe were responsible for this behavior.

A list of potential applications for solid lubricant systems capable of working at intermediate temperatures (i.e. up to 600°C) includes gas turbine seals, cylinder wall/piston rings for low heat rejection diesels engines, various furnace components among others [18]. Another important potential application with specific requirements, concerning both μ 's and WRs, as well as good mechanical properties, is air foil bearings [18,19]. In this application, solid lubricants are needed to prevent wear and reduce friction during engine start-up and shut-down [19]. In foil bearing applications, the higher the temperature at which they run, the less need for cooling and the more efficient they become.

The goal of this work is to understand the tribological behavior of predominantly single-phase MAX samples, and evaluate them as potential triboactive materials, especially for high-temperature tribological applications in general, and as enabling materials in foil bearing technology, in particular. In this work, we report on the tribological behavior at 26 and 550°C of the following layered ternary carbides: Ti_2AlC , Cr_2AlC , Ta_2AlC , Ti_3SiC_2 , Ti_2AlN , Ti_4AlN_3 , Cr_2GeC , Cr_2GaC , Nb_2SnC and Ti_2SnC , tested against Ni-based superalloys, which are widely used as high-temperature engineering materials.

2. Experimental details

The Ti_2AlC , Ti_2AlN and Cr_2AlC samples were obtained from 3-ONE-2, Voorhees, NJ. The processing parameters for synthesizing Ti_3SiC_2 , Ti_2SnC , Nb_2SnC , Ti_4AlN_3 , and Cr_2GaC are summarized in Table 1. The processing details can be found elsewhere [4,20,21]. Table 2 lists the sources of materials and powders used.

To fabricate the Cr_2GeC samples stoichiometric amounts of Cr, Ge and C powders were ball milled for 1 h. The powders were cold-pressed and annealed at 800°C for 10 h. The annealed precursors were then uniaxially hot-pressed in a BN sprayed graphite die under a stress of 40 MPa at 1375°C for 6 h.

The friction and wear tests were performed using a high-temperature pin-on-disc tribometer (CSM, Switzerland) capable of going up to 600°C . All the testing was done at a linear velocity of 1 m/s and a load of 3 N. The sliding distance at room temperature varied from 300 to 800 m; at 550°C it was at least 2 km.

The MAX-based samples were shaped into cuboid chip having a square 6 mm \times 6 mm working face ~ 2 mm thick. The counter surfaces were 9.5 mm thick superalloy (SA) cylindrical (55 mm diameter) discs of Inconel718 or Inconel-600 (High Temp Metals, Inc., Sylmar, CA), henceforth referred to as Inc718 and Inc600, respectively. The base composition of Inc718 is Ni 50–55% Cr 22–24% Fe 20–23% (wt.%), with small (<5 wt.%) quantities of additions like Nb, C, Mo, Si, Mn, Si, etc. For simplicity herein we assume the chemistry of Inc718 to be close to Ni:Cr:Fe $\approx 0.5:0.25:0.25$. Similarly, the base composition of Inc600 is Ni 70–75% Cr 15–17% Fe 6–10% (wt.%), with small (<2 wt.%) quantities of additions like C, Si, Mn, Cu, etc. therefore its chemistry is, approximately, Ni:Cr:Fe $\approx 0.7:0.2:0.1$.

Table 1
Summary of MAX phase microstructures

Compo-sition	Process	Parameters	Grain size	Secondary phases
Ti_2AlC	3-ONE-2		$\approx 45 \mu\text{m}$	Ti_3AlC_2 (<3 vol.%) and TiAl_3 (<2 vol.%)
Ti_2AlN			$\approx 20 \mu\text{m}$	Ti_4AlN_3 ($\sim 5\text{--}9$ vol.%); TiN and Al_2O_3 (<1 vol.%)
Cr_2AlC			$\approx 20 \mu\text{m}$	Cr_7C_3 (≈ 3 vol.%) and Al_2O_3 (<1 vol.%)
Ti_4AlN_3	HIP	1275°C for 24 h under 70 MPa	(20–30) μm	TiN (<1 vol.%) and Al_2O_3 (<1 vol.%)
Ti_3SiC_2	HIP	1450°C for 40 h under 40 MPa	$\approx 4 \mu\text{m}$	SiC (≈ 2 vol.%) and TiC (≈ 2 vol.%)
Ta_2AlC	HIP	1600°C for 8 h under 70 MPa	$\approx 20 \mu\text{m}$	TaAlC_3 (≈ 5 vol.%), TaAl_2 (≈ 2 vol.%) and Al_2O_3 (<1 vol.%)
Cr_2GaC	HIP	1200°C for 12 h under 70 MPa	$\approx 30 \mu\text{m}$	Cr_7C_3 (<1 vol.%) and Ga (<1 vol.%)
Ti_2SnC	HIP	1325°C for 4 h under 70 MPa	(5–10) μm	Sn (5 vol.%) and TiC_x (<1 vol.%)
Nb_2SnC	HIP	1300°C 4 h under 70 MPa	(5–10) μm	NbC_x (<1 vol.%) and Sn (4 vol.%)
Cr_2GeC	HP	See text	$\approx 20 \mu\text{m}$	Cr_2O_3 (<3 vol.%) and Ge (<1 vol.%)

Table 2
Characteristics of starting powder precursors

Powder precursors	Source	Particle size	Purity
Ti			99.5%
Cr	Alfa Aesar (Ward Hill, MA)		99%
Nb		–325 mesh	99.80%
Sn	Aldrich (Milwaukee, WI)		99.80%
Ga	Alfa Aesar (Ward Hill, MA)	3 mm pellets	99.99%
Ge		–200 mesh	99.99%
TiN	Advanced Technology Inc., NJ	(2–3) μm	99.8%
AlN		dm \approx 3 μm	32 wt.% (N-min)
Graphite	Alfa Aesar (Ward Hill, MA)	–300 mesh	99%
SiC	Atlantic Eng. Equip. (Bergenfield, NJ)	–400 mesh	99.50%
Ta ₂ AlC	3-ONE-2, Voorhese, NJ.	–325 mesh	> 92%
Cr ₂ AlC	3-ONE-2, Voorhese, NJ	–325 mesh	>95%
Ag	Alfa Aesar (Ward Hill, MA)	–325 mesh	99.9%

All surfaces were polished to a 1 μm diamond finish, washed with acetone and dried prior to testing. The measured μ 's will be referred to in two ways: μ_m to refer to the mean friction coefficient over the entire sliding distance, and μ_s to refer to its steady state value during sliding.

The WRs of the MAX phase samples were determined by measuring their weights before and after testing in a scale with a resolution of 10^{-4} g. The WRs were calculated by normalizing the volumetric wear by the total sliding distance and applied load. The wear of the SA discs was measured by laser profilometry [Solarius Development, Sunnyvale, CA].

Profilometry of the MAX surfaces after testing were carried out by an atomic force microscope AFM (Dimension-3000, Digital Instruments, Santa Barbara, CA) in a scanning mode over a $100 \mu\text{m} \times 100 \mu\text{m}$ contact area and a scan rate of 0.5 Hz. The average root mean square roughness values, R_{RMS} of the scanned surfaces were calculated.

The worn surfaces were also characterized by optical (Olympus PMG-3) and field emission scanning electron microscopy, SEM (XL-30, FEI-Philips, Hillsboro, OR). The chemistries of the tribofilms were evaluated with an energy dispersive spectroscope, EDS (EDAX, Mahwah, NJ) attached to the SEM. During this work on the contact surfaces metastable and/or multi-component regions were formed. To call these regions phases would be a gross oversimplification and in many cases would be incorrect. So, the chemistries – determined by EDS analysis – of the regions designated by letters in the various SEM micrographs as well as in the tables, will be designated as between two asterisks, viz. *microconstituent*. In most cases, it was not possible to quantify carbon by EDS analysis and its exact value is unknown and thus designated as x.

The volume fractions of the binary carbides, which are almost always present in the ternaries, were determined from image analysis of SEM backscattered, BS, micrographs. The grain size was calculated by a linear intercept of at least 10 grains. Since the MAX phase-grains tend to grow as hexagonal plates, what is reported is the average diameters of the plates.

The volume fractions of un-reacted A-group elements, such as Sn and Ga, present in some of the compositions, were

determined using a differential scanning calorimeter, DSC [Perkin-Elmer, Boston MA]. The details can be found elsewhere [22].

X-ray diffraction, XRD, patterns were obtained on a Siemens D500 diffractometer (Bruker AXS, Madison, WI) using Cu K α radiation, step scan 0.02° , 1 s per step. When possible, Si powders were used as an internal standard.

3. Results

3.1. Synthesis and microstructure

A summary of the purities and grain sizes of the ternary carbides investigated herein (Table 1) clearly show that the least pure sample was 90 vol.% pure, with many much purer. The Cr₂GeC sample, synthesized here for the first time, was \approx 95 vol.% pure; it contained \sim 4 vol.% Cr₂O₃ and \sim 1 vol.% Ge as impurity phases. Its average grain size was \approx 20 μm .

3.2. Room temperature results

At ambient temperature, for all the MAX samples tested, the initial μ 's were low (<0.1 – 0.2), but rapidly increased to values >0.5 (Table 3). Typical variations of the μ 's as a function of sliding distance are represented in Fig. 1a and b, showing the μ 's

Table 3
Summary of WR and μ of different tribocouples at 26 °C and 3 N load

Specimen	Dynamic partner	WR of MAX ($\text{mm}^3/\text{N}\cdot\text{m}$)	μ_{mean}
Ti ₂ AlC	Inc718	$\approx 5.5 \times 10^{-4}$	0.5 ± 0.1
Ti ₂ AlN	Inc718	$\approx 3 \times 10^{-2}$	0.8 ± 0.15
Ti ₄ AlN ₃	Inc718	$\approx 3 \times 10^{-2}$	0.8 ± 0.15
Ti ₃ SiC ₂	Inc718	$\approx 2.5 \times 10^{-2}$	0.6 ± 0.15
Cr ₂ AlC	Inc718	$\approx 1.2 \times 10^{-3}$	0.6 ± 0.1
Ta ₂ AlC	Inc718	$\approx 1.5 \times 10^{-2}$	0.5 ± 0.1
Cr ₂ GeC	Inc600	$\approx 1.2 \times 10^{-3}$	0.5 ± 0.1
Cr ₂ GaC	Inc600	$\approx 4 \times 10^{-2}$	0.4 ± 0.1
Ti ₂ SnC	Inc600	$\approx 8 \times 10^{-3}$	0.63 ± 0.1
Nb ₂ SnC	Inc600	$\approx 1.5 \times 10^{-2}$	0.63 ± 0.1

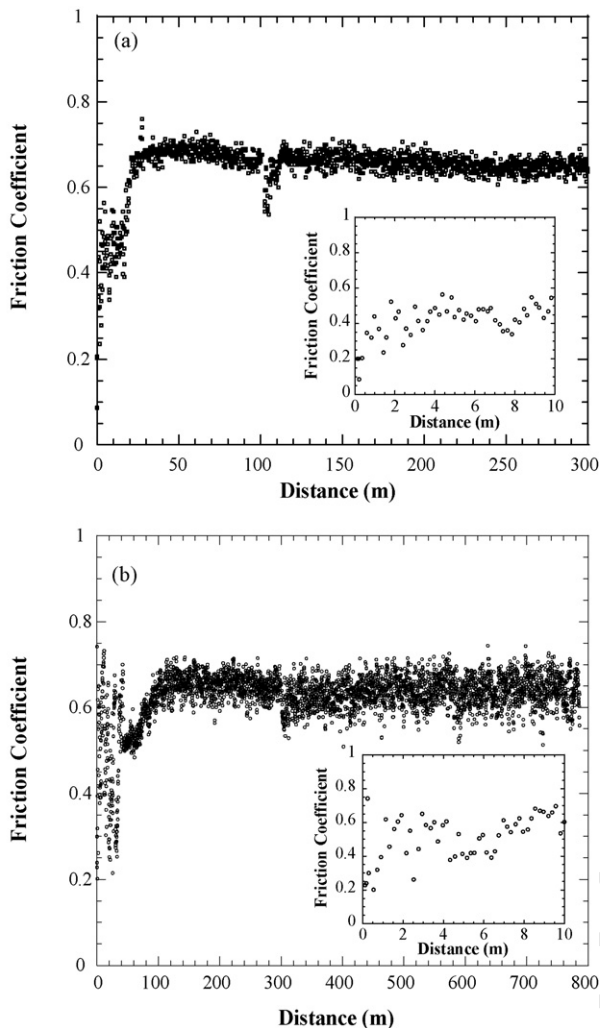


Fig. 1. Change in μ as a function of sliding distance at 26 °C, when Inc718 was tested against, (a) Ti_3SiC_2 and (b) Ta_2AlC . In both (a) and (b), insets show evolution of μ 's during initial 10 m.

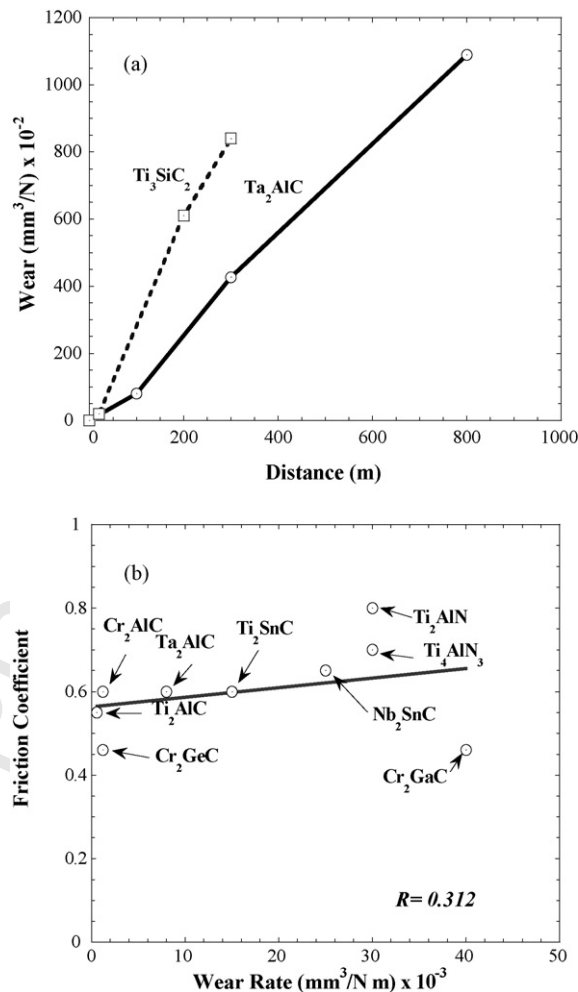


Fig. 2. (a) Typical plot of wear of Ti_3SiC_2 and Ta_2AlC as a function of sliding distance against Inc718; (b) wear rate versus μ 's after dry sliding against Inc718. A linear regression line was fitted (solid line) to the data points; the correlation coefficient, R , is shown.

versus sliding distance for Ti_3SiC_2 and Ta_2AlC tested against Inc718. Fig. 2a plots the absolute wear for Ti_3SiC_2 and Ta_2AlC versus sliding distance. The almost linear dependencies reveal that the WRs are more or less constant with sliding distance.

At $\geq 10^{-4} \text{ mm}^3/\text{N}\cdot\text{m}$, the WRs of all the MAX phases were high, irrespective of the counter surface used (Table 3). No correlation was found between the WRs and the μ 's (Fig. 2b). From the profilometry and the microscopy results, the WRs of the SA surfaces were low and difficult to quantify.

Typical SEM micrographs of the $\text{Ta}_2\text{AlC}/\text{Inc718}$ worn surfaces, shown in Fig. 3, showed to be covered with pulverized, partially oxidized, wear particles of an average composition, $A = *[\text{Ta}_{0.7}\text{Al}_{0.3}]\text{O}_{0.1}\{\text{C}_x\}$ *. At the same time, a smeared discontinuous transfer film – observed on the Inc718 surfaces (Fig. 3b) – had an average composition, $B = *[\text{Ta}_{0.66}\text{Al}_{0.33}]\text{O}_{0.3}\{\text{C}_x\}$ * (Table 4). Sliding marks were also observed on the Inc718 surfaces (Fig. 3b).

Table 4
Average chemistries of areas labeled in Figs. 3, 5 and 6 as determined by EDS analysis

Region	Surface examined	Wear partner	*Average composition*
A (Fig. 3a)	Ta_2AlC	Inc718	$[\text{Ta}_{0.7\pm 0.04}\text{Al}_{0.3\pm 0.03}]\text{O}_{0.1\pm 0.04}\{\text{C}_x\}$
B (Fig. 3b)	Inc718	Ta_2AlC	$[\text{Ta}_{0.66\pm 0.04}\text{Al}_{0.33\pm 0.02}]\text{O}_{0.3\pm 0.02}\{\text{C}_x\}$
C (Figs. 5 and 6a)	Ta_2AlC Inc718	Inc718 Ta_2AlC	$[\text{Ta}_{0.09\pm 0.07}\text{Al}_{0.01\pm 0.01}\text{Ni}_{0.5\pm 0.15}\text{Cr}_{0.2\pm 0.1}\text{Fe}_{0.2\pm 0.1}]\text{O}_{0.7\pm 0.14}$
D (Fig. 6b)	Inc718	Ti_3SiC_2	$[\text{Ni}_{0.25\pm 0.03}\text{Cr}_{0.1\pm 0.01}\text{Fe}_{0.1\pm 0.01}\text{Ti}_{0.35\pm 0.05}\text{Si}_{0.2\pm 0.03}]\text{O}_{1.2\pm 0.05}$
E (Fig. 6c)	Inc718	Cr_2AlC	$[\text{Ni}_{0.5\pm 0.01}\text{Cr}_{0.25\pm 0.03}\text{Fe}_{0.25\pm 0.03}]\text{O}_{1\pm 0.05}$
F (Fig. 6d)	Inc718	Ti_2AlC	$[\text{Ni}_{0.55\pm 0.05}\text{Cr}_{0.23\pm 0.03}\text{Fe}_{0.22\pm 0.03}]\text{O}_{0.9\pm 0.2}$

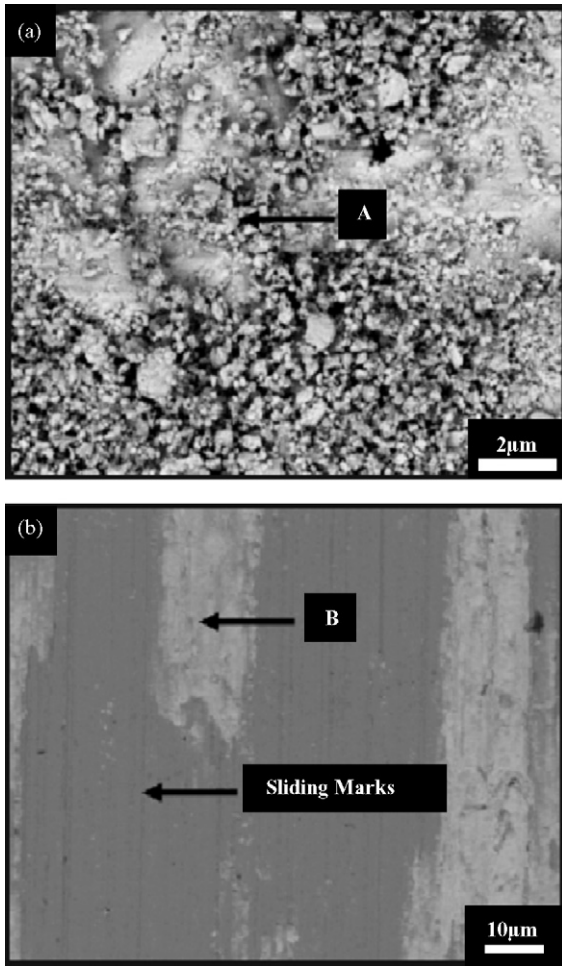


Fig. 3. BSE SEM micrographs of tribosurfaces after dry sliding of Ta₂AlC against Inc718 at 26 °C: (a) Ta₂AlC surface and (b) Inc718 surface. Compositions of μ Cs designated by letters are listed in Table 4.

3.3. High-temperature results

When tested against the SAs at 550 °C, the μ_s 's for all the MAX phases were <0.5 (Table 5). Typical examples are shown in Fig. 4a and b, where the dependencies of μ on sliding distance for Ti₃SiC₂ and Ta₂AlC, respectively, are plotted. Interestingly, initially when the values of μ are high (\sim 0.6) the tribocouples were accompanied by a loud metallic noise; once the μ 's

Table 5
Summary of μ and WRs of different tribocouples at 550 °C

Static partner	Dynamic partner	WR _s (mm ³ /N-m)	WR _d (mm ³ /N-m)	μ_s
Ta ₂ AlC	Inc718	$\leq 1 \times 10^{-6}$	$\sim 10^{-5}$	≈ 0.4
Ti ₃ SiC ₂		$\leq 1 \times 10^{-6}$		≈ 0.4
Cr ₂ AlC		$\leq 1 \times 10^{-6}$	$\sim 10^{-5}$	≈ 0.3
Ti ₂ AlC		$\leq 1 \times 10^{-6}$		≈ 0.4
Cr ₂ GaC	Inc600	$\approx 5 \times 10^{-4}$		≈ 0.5
Cr ₂ GeC	Inc600	$\approx 6 \times 10^{-6}$		≈ 0.35
Ti ₂ AlN	Inc718	$\approx 3 \times 10^{-5}$		≈ 0.4
Ti ₄ AlN ₃	Inc600	$\approx 1 \times 10^{-3}$		≈ 0.6

Note: WR_s – specific wear rate of the static tribo-partner. WR_d – specific wear rate of the dynamic tribo-partner.

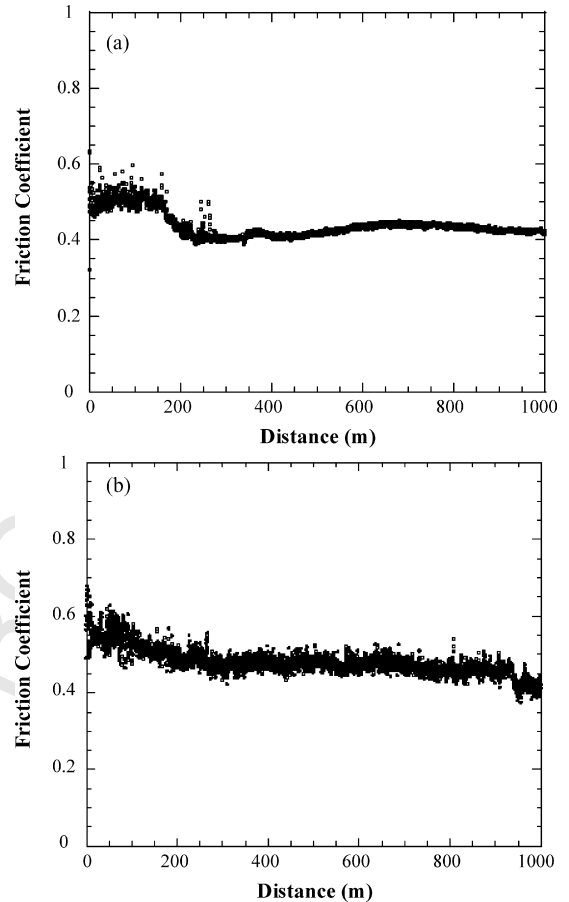


Fig. 4. Change in μ as a function of sliding distance when, (a) Ti₃SiC₂ and (b) Ta₂AlC were tested against Inc718 at 550 °C.

decreased to their steady state values of \sim 0.4, the tribo-noises were significantly reduced.

Most of the MAX phases tested against the SAs at 550 °C showed negligible ($\leq 10^{-5}$ mm³/N-m) WRs after 2 km of sliding (Table 5). The high WRs observed for the Cr₂GaC sample are most probably related to the presence of Ga excess at the grain boundaries.

Based on this preliminary work, it was concluded that the tribocouples of Ta₂AlC, Ti₃SiC₂, Cr₂AlC and Ti₂AlC with Inc718 were the most promising. Accordingly extensive EDS and profilometric studies were carried out to characterize their tribosurfaces after testing.

After sliding against Inc718 at 550 °C for 2 km, the Ta₂AlC surfaces (Fig. 5a) were covered with oxidized tribofilms of average composition, $C = *[\text{Ni}_{0.45}\text{Fe}_{0.22}\text{Cr}_{0.23}\text{Ta}_{0.1}]\text{O}_{0.7}$ *. Even at higher magnifications, the tribofilms formed appeared dense and smooth; no evidence of phase separation was observed (Fig. 5b). Weak C peaks were present in some of the EDS spectra, but, here again, it was impossible to quantify them and C is thus not included in the chemistries listed.

The Inc718 surfaces were slightly gouged and covered with sporadic and discontinuous tribofilms (Fig. 6a). Under the optical microscope, OM, these areas were colored metallic gray (inset in Fig. 6a). EDS of the tribofilms identified them to be an oxide with an average composition $\approx C$ (Table 4). Analogously,

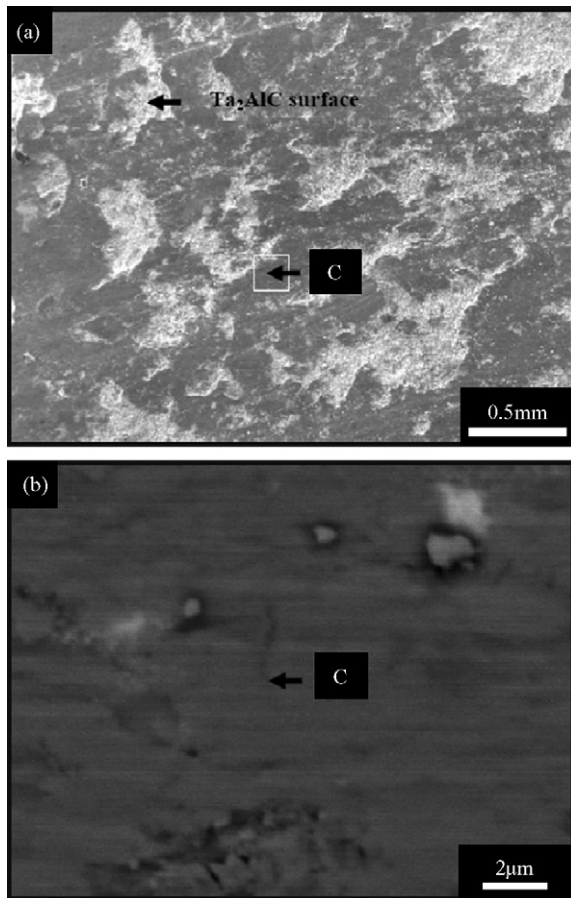


Fig. 5. SEM micrographs showing tribofilms formed on Ta₂AlC surface after dry sliding for 2 km against Inc718 at 550 °C, (a) SE image and (b) higher magnification BSE image of the region marked with a rectangle in (a).

no phase separation in these oxide layers was observed (inset in Fig. 6a).

Similar observations were made on the Inc718 surfaces after 2 km of sliding against Ti₃SiC₂ (Fig. 6b), Ti₂AlC (Fig. 6c) and Cr₂AlC (Fig. 6d). In all cases, the Inc718 surfaces were slightly gouged and covered by patchy tribofilms. These tribofilms were also significantly oxidized, and their main constituents reflected

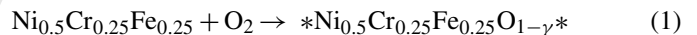
the SA chemistry (Table 4). Laser profilometry of the worn Inc718 surfaces after testing against Cr₂AlC (Fig. 7a) and Ta₂AlC (Fig. 7b) detected tribofilms and gouges of the order of a few micrometers, corroborating the microscopy results. Because of the stochastic nature of the gouging and tribofilms, it was difficult to quantify the wear of the Inc718 substrates. Nevertheless, a semi-quantitative estimation was carried out (see Appendix A) based on the profilometric data. The WRs estimated for the SA surfaces examined were all of the order of $\sim 10^{-5}$ mm³/N-m (Table 5).

The post-sliding roughness of the MAX surfaces – analyzed with an AFM – was found to be extremely smooth (Fig. 8). The R_{RMS} of Ta₂AlC (Fig. 8), Cr₂AlC, Ti₃SiC₂ and Ti₂AlC (not shown) surfaces were determined to be about 350 nm, 325 nm, 540 nm and 272 nm, respectively.

The X-ray diffraction patterns of the surfaces of Ta₂AlC samples after 2 km sliding against Inc718 did not reveal any new details compared to the bulk material.

4. Discussion

Before discussing the room temperature results, it is instructive to discuss the high-temperature ones. When the MAX surfaces are in contact with Ni-based SAs at 550 °C, tribofilms form on both contact surfaces (Figs. 5a and 6). These tribofilms are X-ray amorphous or nanocrystalline. According to EDS analysis (Table 4), they are mainly comprised of partially oxidized SA constituents, viz.:



with $\gamma \leq 0.5$. These tribooxides apparently smear onto and coat the MAX-surfaces (e.g. region C in Fig. 5). In some cases, small amounts of elements from the MAX phases are found in the SA tribosurfaces (e.g. phases C and D in Table 4). As summarized in Table 5, these tribooxides result in relatively low μ 's (< 0.4) and quite low WRs ($\leq 10^{-6}$ mm³/N-m).

That these oxides are lubricious is not too surprising. In the literature, it is known that Ni-based binary alloys, e.g. Ni-2Ta, Ni-20W, Ni-20Cu, display μ 's ~ 0.6 when sliding against Al₂O₃

Table 6
Effect of interfacial film chemistries on μ

Solid lubricant	Temperature (°C)	μ_s	Reference
[Ni _{0.45} Fe _{0.22} Cr _{0.23} Ta _{0.1}]O _{0.7}	550	0.3–0.5	Present work
[Ni _{0.25} Fe _{0.1} Cr _{0.1} Ti _{0.35} Si _{0.2} C _x]O _{1.2}			
[Ni _{0.5} Fe _{0.25} Cr _{0.25}]O ₁			
[Ni _{0.55} Fe _{0.22} Cr _{0.23}]O _{0.9}			
ZnO	600	0.7	[25]
NiO	500–800	0.4–0.6	
FeO	300–800	0.6	
CoO	300–600	0.4–0.6	
NiO–FeO	600	0.6	
NiO–TiO ₂	400–800	0.3–0.5	
Ti ₅ O ₉	400	0.8	[26]
Ti ₉ O ₁₇ , γ -Ti ₃ O ₅ , Ti ₉ O ₁₇ , NiTiO ₃	800	0.2–0.8	
Si _x O _y	400	0.7	
SiN _x O _y	800	0.6–0.8	

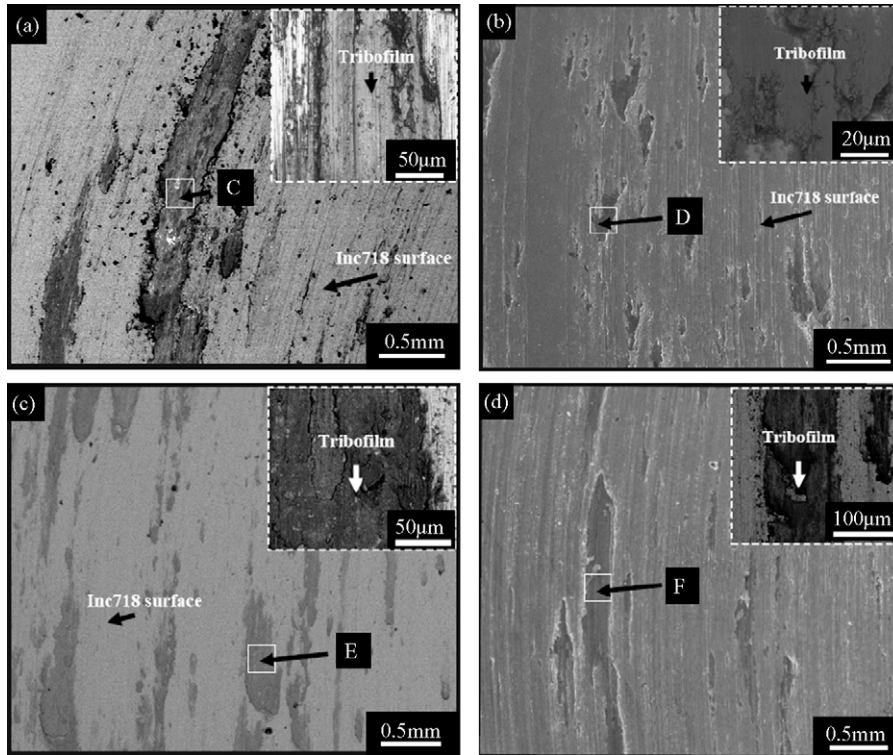


Fig. 6. SEM micrograph of tribofilms formed on Inc718 surfaces after 2 km dry sliding at 550 °C against, (a) Ta₂AlC (BSE). Inset shows an optical micrograph of the tribofilm (light blue), (b) Ti₃SiC₂ (SE). Inset shows the SEM micrograph (BSE) at higher magnification, (c) Cr₂AlC (BSE). Inset shows the BSE SEM micrograph at higher magnification, (d) Ti₂AlC (SE). Inset shows the BSE SEM micrograph of the tribofilm.

at 26 °C. As the temperature is increased, μ drops to 0.3–0.4 because of the formation of lubricious oxides, like NiO [24,25]. It is also established that several transition metal oxides, e.g. ZnO, FeO, etc. can be used as solid lubricants at elevated temperatures (Table 6) [25]. It is thus reasonable to assume that in this work Ni-based lubricious tribooxides are generated, and that these oxides transfer onto the MAX phase surfaces, leading to the low WRs and μ 's.

The results of Hongxiang et al. [17] – who studied Ti₃AlC₂ by a block-on-disc method against low carbon steel at 0.8 MPa, but at very high rotation speeds (60 m/s), observed a $\mu \sim 0.1$ and specific WRs $\sim 2.5 \times 10^{-6}$ mm³/N-m – are also consistent with our interpretation. In that work the excellent tribological properties were ascribed to the formation of self-generating tribofilms, composed of Ti, Al, Fe and O. In their case, the tribooxides formed at room temperature, presumably as a result of the increased contact temperatures at the high rotation speeds used.

In light of these conclusions, what is occurring at room temperature becomes clear. At room temperatures, tribooxides either do not form or they form, but are too brittle or thin to impart any lubricity. What seems to occur instead is the formation of massive wear particles, which are presumably quite abrasive, resulting in the high WRs observed (Table 3). Interestingly these third body particles are slightly oxidized (Table 4). Consistent with this notion is the fact that high-temperature lubricious oxides, like NiO and ZnO, are brittle at room temperature [25]. How this problem was

solved by the addition of Ag is discussed in a forthcoming paper.

It is appropriate to note here the tribological study of Ti₃SiC₂ against steel by Souchet et al. [15], who showed that as long as a tribofilm comprised of Ti, C and O was maintained between the pin and disk, the tribological properties were excellent. Disruption of that film resulted in high μ 's and WRs. Also noteworthy was that when the same tribocouple was tested in vacuum at room temperature, the initial low WRs and low μ stage was absent. Both observations support our arguments about the key role oxygen plays in enhancing the tribological properties of the MAX/SA tribocouples.

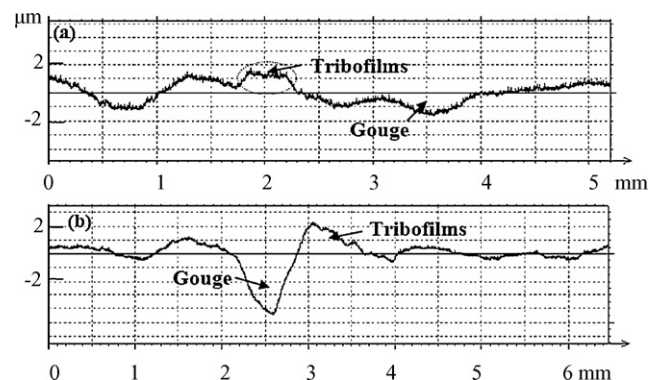


Fig. 7. Laser profilometry on Inc718 surfaces after dry sliding for 2 km at 550 °C against, (a) Cr₂AlC and (b) Ta₂AlC.

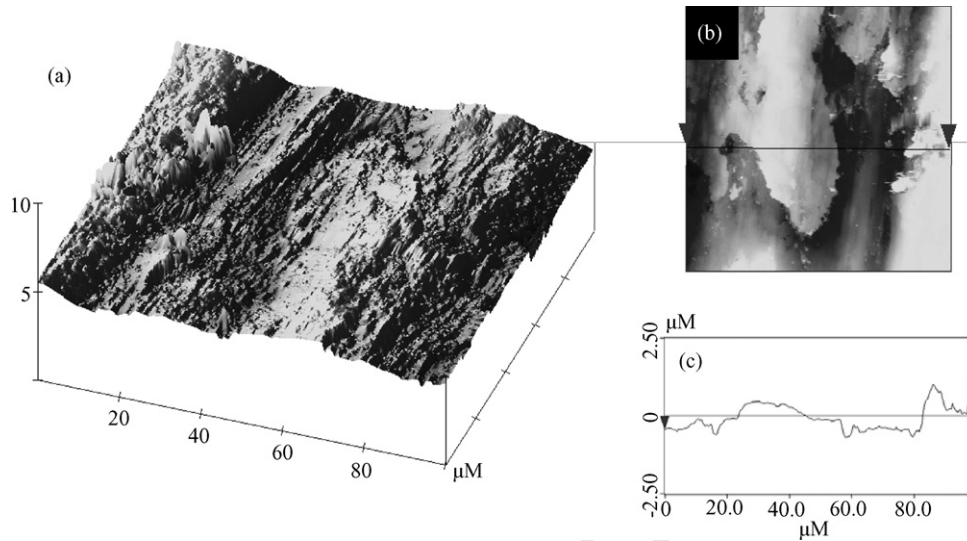


Fig. 8. AFM analysis in scanning mode on $100\ \mu\text{m} \times 100\ \mu\text{m}$ Ta_2AlC surface after testing against Inc718 for 2 km sliding at $550\ ^\circ\text{C}$, (a) isometric view, (b) top view and (c) side view of the profile of the region marked by arrows in top view.

5. Conclusions

At room temperature, when tested against SAs, the tribological behavior of the MAX phases were characterized by μ 's > 0.4 and high WRs ($\geq 10^{-4}\ \text{mm}^3/\text{N}\cdot\text{m}$). Third body abrasion is believed to be responsible for this behavior.

In contradistinction, at $550\ ^\circ\text{C}$ the MAX/Inc718 tribocouples form lubricious tribooxide films, comprised mainly of oxides of the superalloy elements, viz. Ni, Fe and Cr. The formation of this lubricious tribofilms at the contact areas is believed to be responsible for the ultra-low wear rates of the MAX phases ($< 10^{-6}\ \text{mm}^3/\text{N}\cdot\text{m}$) and the slightly higher WR's of the Inc718 surfaces ($\sim 10^{-5}\ \text{mm}^3/\text{N}\cdot\text{m}$) as well as the relatively low μ 's (< 0.4).

Uncited reference

[23]

Acknowledgement

This work was supported by ONR (N00421-03-C-0085).

Appendix A. Estimation of WR of SA counterparts

If one assume the average gouge is of uniform depth throughout the tested wear track, i.e. $\sim 0.5\ \mu\text{m}$ for the Inc718 counterpart after the 2 km sliding against Ta_2AlC at $550\ ^\circ\text{C}$ (Fig. 7b), then the volume of worn material is $0.018\ \text{mm}^3$ on a $36\ \text{mm}^2$ area in the track. For the given volume of worn material WR could be estimated by the formula (A.1):

$$\text{WR} = \frac{V_w}{(F_n l_s (L/2\pi r_{\text{mean}}))} \quad (\text{A.1})$$

where V_w : volume of worn material, F_n : normal load, l_s : linear tab size, L : sliding distance and r_{mean} : mean track radius.

The normal load is 3 N, using r_{mean} (mean radius of track) $\sim 10\ \text{mm}$, 6 mm sample length, and using the formula (A.1), the WR of the Inc718 could be estimated as $\sim 10^{-5}\ \text{mm}^3/\text{N}\cdot\text{m}$.

The similar value of $\sim 10^{-5}\ \text{mm}^3/\text{N}\cdot\text{m}$ was obtained by analogous calculations of the WR of the Inc718 counterpart tested against Cr_2AlC at $550\ ^\circ\text{C}$ (Fig. 7a), $r_{\text{mean}} \sim 12\ \text{mm}$.

References

- [1] M.W. Barsoum, M. Radovic, in: R.W.C.K.H.J. Buschow, M.C. Flemings, E.J. Kramer, S. Mahajan, P. Veysiere (Eds.), Encyclopedia of Materials Science and Technology, Elsevier, Amsterdam, 2004.
- [2] M.W. Barsoum, T. El-Raghy, Synthesis and characterization of a remarkable ceramic: T_3SiC_2 , J. Am. Ceram. Soc. 79 (1996) 1953–1956.
- [3] M.W. Barsoum, The $\text{M}_{N+1}\text{AX}_N$ phases: a new class of solids; thermodynamically stable nanolaminates, Prog. Solid State Chem. 28 (2000) 201–281.
- [4] M. Radovic, M.W. Barsoum, T. El-Raghy, S.M. Wiederhorn, W.E. Luecke, Effect of temperature, strain rate and grain size on the mechanical response of T_3SiC_2 in tension, Acta Mater. 50 (2002) 1297–1306.
- [5] T. El-Raghy, M.W. Barsoum, A. Zavaliangos, S.R. Kalidindi, Processing and mechanical properties of T_3SiC_2 . II. Effect of grain size and deformation temperature, J. Am. Ceram. Soc. 82 (1999) 2855–2860.
- [6] T. Zhen, M.W. Barsoum, S.R. Kalidindi, M. Radovic, Z.M. Sun, T. El-Raghy, Compressive creep of fine and coarse-grained T_3SiC_2 in air in the $1100\text{--}1300\ ^\circ\text{C}$ temperature range, Acta Mater. 53 (2005) 4963–4973.
- [7] S. Gupta, M.W. Barsoum, Synthesis and oxidation of V_2AlC and $(\text{Ti}_{0.5}, \text{V}_{0.5})_2\text{AlC}$ in air, J. Electrochem. Soc. 151 (2004) D24–D29.
- [8] M.W. Barsoum, N. Tzenov, A. Procopio, T. El-Raghy, M. Ali, Oxidation of $\text{Ti}_{n+1}\text{AlX}_n$ ($n = 1\text{--}3$ and $X = \text{C}, \text{N}$). II. Experimental results, J. Electrochem. Soc. 148 (2001) C551–C562.
- [9] X.H. Wang, Y.C. Zhou, Oxidation behavior of T_3AlC_2 powders in flowing air, J. Mater. Chem. 12 (9) (2002) 2781–2785.
- [10] S. Myhra, J.W.B. Summers, E.H. Kisi, T_3SiC_2 – a layered ceramic exhibiting ultra – low friction, Mater. Lett. Mater. Lett. 39 (1999) 6–11.
- [11] T. El-Raghy, P. Blau, M.W. Barsoum, Effect of grain size on friction and wear behavior of T_3SiC_2 , Wear 238 (2) (2000) 125–130.
- [12] Z.M. Sun, Y.C. Zhou, S. Li, Tribological behavior of T_3SiC_2 -based material, J. Mater. Sci. Technol. 18 (2002) 142–145.
- [13] Y. Zhang, G.P. Ding, Y.C. Zhou, B.C. Cai, T_3SiC_2 —a self-lubricating ceramic, Mater. Lett. 55 (2002) 285–289.

- 382 [14] H.Z. Zhai, Z.Y. Huang, Y. Zhou, Z.L. Zhang, Y. Wang, M. Al, Oxidation
383 layer in sliding friction surface of high-purity Ti_3SiC_2 , *J. Mater. Sci.* 39
384 (21) (2004) 6635–6637.
- 385 [15] A. Souchet, J. Fontaine, M. Belin, T. Le Mogne, J.-L. Loubet, M.W.
386 Barsoum, Tribological duality of Ti_3SiC_2 , *Tribol. Lett.* 18 (2005) 341–
387 352.
- 388 [16] D. Sarkar, B. Basu, S.J. Cho, M.C. Chu, S.S. Huang, S.W. Park, Tribological
389 properties of Ti_3SiC_2 , *J. Am. Ceram. Soc.* 88 (11) (2005) 3245–3248.
- 390 [17] Z. Hongxiang, H. Zhenying, A. Zingxing, Z. Yang, Z. Zhilli, L. Shibo,
391 Tribophysical properties of polycrystalline bulk Ti_3AlC_2 , *J. Am. Ceram.*
392 *Soc.* 88 (11) (2005) 3270–3274.
- 393 [18] C. Dellacorte, H.E. Sliney, Tribological Properties of PM212: A High-
394 Temperature, Self-Lubricating, Powder Metallurgy Composite, NASA TM
395 102355, 1990.
- 396 [19] C. Dellacorte, A. Zaldana, K. Radil, A systems approach to the solid lubri-
397 cation of foil air bearings for oil-free turbomachinery, *J. Tribol.* 126 (2004)
201–207.
- [20] T. El-Raghy, S. Chakraborty, M.W. Barsoum, Synthesis and characteriza- 398
tion of Hf_2PbC , Zr_2PbC and M_2SnC ($M = Ti, Hf, Nb$ or Zr), *J. Eur. Ceram.* 399
Soc. 20 (2000) 2619. 400
- [21] Z.M. Sun, S. Gupta, H. Ye, M.W. Barsoum, Spontaneous growth of free- 401
standing Ga nanoribbons from Cr_2GaC surfaces, *J. Mater. Res.* 20 (2005) 402
2618–2621. 403
- [22] A.T. Procopio, M.W. Barsoum, T. El-Raghy, Synthesis of Ti_4AlN_3 and 404
phase equilibria in the Ti-Al-N system, *Metall. Mater. Trans. A* 31A (2000) 405
333–337. 406
- [23] S. Gupta, D. Filimonov, M.W. Barsoum, Isothermal oxidation of Ta_2AlC 407
in air, *J. Am. Ceram. Soc.* 89 (2006) 2974–2976. 408
- [24] M.B. Peterson, S.J. Calabrese, S. LI, X. Jiang, Friction of alloys at high 409
temperature, *J. Mater. Sci. Technol.* 10 (1994) 313–320. 410
- [25] A. Erdemir, *Modern Tribology Handbook*, CRC Press LLC, 2003, Chapter 411
22. 412
- [26] A. Skopp, M. Woydt, Ceramic and ceramic composite materials with 413
improved friction and wear properties, *Tribol. Trans.* 38 (1995) 233–242. 414

UNCORRECTED PROOF